Resistivities and band structures of alkaline-earth-pnictide systems

1993 J. Phys.: Condens. Matter 5 7551

(http://iopscience.iop.org/0953-8984/5/41/003)

J. Phys.: Condens. Matter 5 (1993) 7551–7562. Printed in the UK

Resistivities and band structures of alkaline-earth–pnictide systems

R Xu†, R A de Groot‡ and W van der Lugt†

† Solid State Physics Laboratory, Materials Science Centre, University of Groningen, Nijenborgh 4, 9747 AG Groningen, The Netherlands

‡ Research Institute for Materials, Faculty of Science, University of Nijmegen, Toernooiveld, 6525 ED Nijmegen, The Netherlands

Received 7 July 1993

Abstract. The electrical resistivities ρ of the liquid Sr–Bi and Sr–Sb alloys have been determined for compositions covering the whole concentration range. Plotted as a function of composition the results resemble those obtained previously for Mg–Bi by other authors. There is a very sharp resistivity maximum at 60 at.% Sr, well up into the semiconducting range. The band structure of solid Mg_3Bi_2 has been calculated using the augmented spherical wave (ASW) method. No gap has been found and it is concluded that solid Mg_3Bi_2 is metallic, in agreement with measurements found in the literature dating from the thirties and before. These measurements were checked and extended through the melting point. Finally, a band-structure calculation was carried out for Mg_3Sb_2, which is a semiconductor in the crystalline as well as in the liquid state.

1. Introduction

Liquid Mg_3Bi_2 is a classical example of a liquid semiconductor [1–3]. It is characteristic that the electrical conductivity of liquid Mg–Bi alloys, plotted as a function of composition, falls extremely steeply near the stochiometric composition. Enderby and Collings [3] mention a minimum value of 45 Ω^{-1} cm^{-1}, as well as a node in the thermopower at the same composition, both indicating a metal–non-metal transition in this system. The thermodynamic properties of liquid Mg–Bi have been studied by Egan [4]. An inflection point in the activity coefficient of Mg was observed around the composition corresponding to Mg_3Bi_2. This corresponds to a sharp peak in the Darken stability function [5]. The liquid structure has been investigated by Weber *et al* [6] and by Boos and Steeb [7], by means of neutron diffraction. They showed that strong short-range order exists in the liquid, particularly at the stoichiometric composition.

Liquid Mg–Bi is an example of a strongly compound-forming alloy system with a well defined stoichiometric composition. Experimental and theoretical work on alloys of alkali metals with post-transition group III, IV, and V elements suggests that in such systems the electronic and geometrical structure of the compound are strongly dependent on r^+/r^-, where r^+ is the size of the electropositive element and r^- that of the electronegative element [8]. Most of these alloys are strongly ionic. More particularly it was shown that for large values of r^+/r^- anion clustering is likely to take place. Moreover the resistivities increase strongly with r^+/r^-. For reviews of this work the reader is referred to [8] and [9].

Though the difference of the electronegativities of Mg and Bi (0.7 on the Miedema scale) [10] is smaller than for the alkali alloys mentioned above it was considered interesting to investigate whether or not such effects occur also in the alkaline-earth–pnictide alloys.

0953-8984/93/417551+12$07.50

Therefore resistivity measurements on the systems Sr–Bi and Sr–Sb were carried out. Not only is the electronegativity difference much larger (1.75 and 2.0, respectively) in these systems, but also the size ratio is larger, making them more similar to the previously investigated alkali-based alloys.

As we will demonstrate below the behaviour of Sr–Bi and Sr–Sb proves to be rather similar to that of Mg–Bi. In order to investigate more closely the mechanisms behind the compound formation and the metal–non-metal transition, a band-structure calculation of solid Mg_3Bi_2 was carried out, as the structures of solid Sr_3Bi_2 and Sr_3Sb_2 are not known. To our surprise, according to the calculations the solid material proved to be metallic. An extensive literature search revealed that this had already been observed experimentally during the thirties and before [11, 12]. It can also be concluded from more recent measurements on amorphous materials [13–15]. To check the older data and to extend them to higher temperatures we performed measurements of the resistivity of Mg_3Bi_2 in the solid state from 500 °C to the melting point. The measurements were continued through the melting point up to 80 °C above the liquidus. They confirm the picture that had gradually developed. Finally we compared our results to those recently obtained by Verbrugge and van Zytveld [16] for the strongly related system Mg–Sb. A band-structure calculation was also carried out for Mg_3Sb_2.

Above we have given an almost chronological account of the investigations. Details will be given in the following sections in approximately the same order.

2. Experiments on the liquid alloys

Bi ingots, nominally 99.999 wt% pure, were obtained from Ventron GmbH. Sb shots with a nominal purity of 99.999 wt% were purchased from Highways Company. Mg ingots with nominal purity of at least 99.98 wt% were supplied by Koch-Light Laboratories Ltd. Sr ingots with a nominal purity of 99.0 wt%, purchased from Highways Company, were delivered in mineral oil. The resistivity measurements on Sr–Bi with Sr concentrations of 0–50 at.% were carried out with the material from Highways. Later Sr from Kawecki-Billiton with nominal purity 99.5 wt% was used. The latter was delivered in the form of rods under Ar. For the other alloys we used material from Kawecki-Billiton. Consistency was checked at a composition of 50 at.% Bi. The resistivities of two samples of pure liquid Sr made from the two supplies proved to be in mutual agreement within the accuracy of the measurements. Also for the Sr–Sb system, Sr from Kawecki-Billiton was used.

In a preliminary phase of the experiments on Sr-Bi we found that the melting point of alloys with an Sr content of 60 at.% made from the Highways material, was poorly determined, but in any case much too high compared to the melting point given in the phase diagram (945 °C) [17]. Moreover the material remained inhomogeneous (i.e. appeared to contain tiny solid particles) up to the highest temperature available to us (1030 °C). The melting point of the 60 at.% Sr alloy with Sr from Kawecki was between 980 °C and 995 °C, much closer to the value (945 °C) quoted in the phase diagram. The problems of preparation and definition are probably related to the method of packing: according to [18] carbides may be formed when the material is kept under mineral oil.

As Sr is a soft metal, the surface could be cleaned with a sharp knife. Preparation and measurements were carried out in an He-filled glove box. Normally, the O_2 content inside the glove box is lower than 1 ppm. For the Sr–Bi system, the metal-tube method was used for the alloys with 0–50 at.% Sr. The experimental set-up was the same as used previously for alkali–Bi systems [19]. In the remaining alloys the high melting point and

the strong evaporation caused serious problems. Therefore a closed-cell method was used. For this method, we refer to [20] and [21]. The accuracy in the temperature is estimated to be ±5 °C; that in the resistivities ±5%.

3. Results for liquid Sr–Bi and Sr–Sb systems

Figure 1 shows the resistivities of liquid Sr–Bi alloys. The temperature dependence of the resistivity is given in figure 2. For clarity of presentation both plots are on a semilogarithmic scale. As a consequence of the evaporation problems no isotherms could be produced.

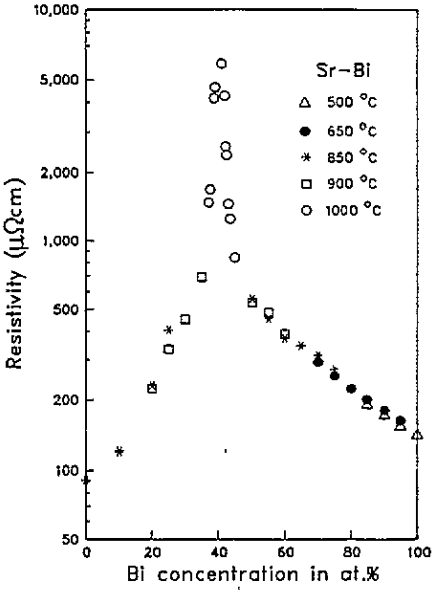

Figure 1. The resistivity ρ of liquid Sr–Bi alloys as a function of composition at the temperatures indicated in the figure.

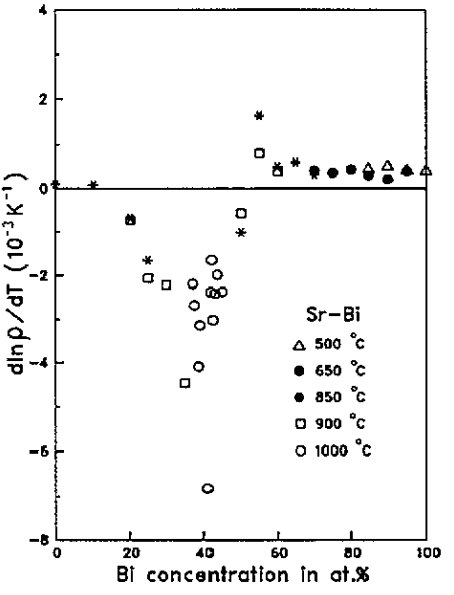

Figure 2. The temperature dependence $d\rho/dT$ of liquid Sr–Bi alloys as a function of composition at the temperatures indicated in the figure.

The resistivity exibits a very sharp peak. The maximum resistivity found by us is 5900 $\mu\Omega$ cm at 1000 °C. This maximum occurs, with an inaccuracy of ±1 at.%, at the octet composition Sr_3Bi_2. The given value of the maximum resistivity is not very reliable and the error is certainly much larger than for the other points. This is not caused by inaccuracies in the determination of the resistivity but by uncertainties in the composition. The peak is very sharp and therefore the resistivities in the vicinity of the peak are extremely sensitive to small deviations from the nominal composition. Such deviations occur easily, first because of unavoidable evaporation, but also because the commmercially obtained Sr had an impurity content of 0.5 %. These impurities are largely other alkaline-earth metals and therefore are not likely to substantially change the position of the maximum, but they may change the resistivity value at the maximum. Such a problem was also encountered in the Mg–Sb system [22].

The resistivity maximum is accompanied by a sharp, negative minimum in the temperature dependence at the same composition as the resistivity maximum. According to

our experiments $d \ln \rho / dT$ amounts to $-6.8\ K^{-1}$ at the position of the minimum, but this value is less reliable for the same reasons that the maximum value of ρ is.

Figure 3 gives the resistivity data for the Sr–Sb system. The overall behaviour is the same as for Sr–Bi but the resistivities are generally higher. The maximum value measured is 7200 $\mu\Omega$ cm, subject to the same reserves as in the case of Sr–Bi. The minimum value of $d \ln \sigma / dT$ is $-5.3\ K^{-1}$ (figure 4).

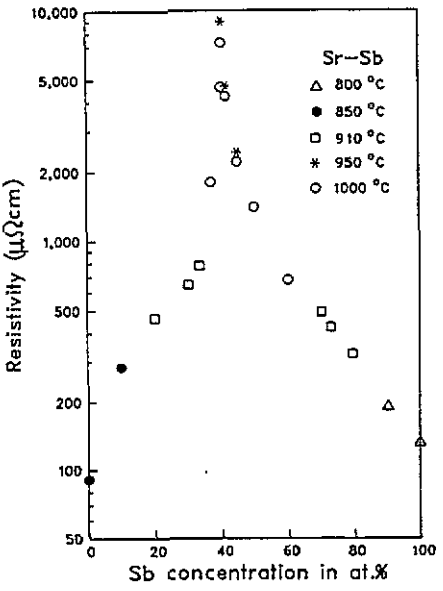

Figure 3. The resistivity ρ of liquid Sr–Sb alloys as a function of composition at the temperatures indicated in the figure.

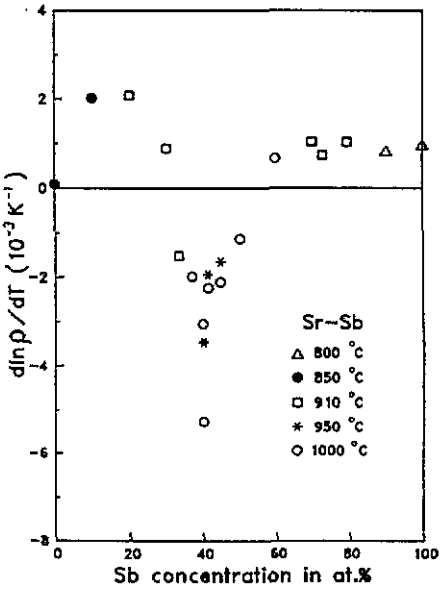

Figure 4. The temperature dependence $d\rho/dT$ of the resistivity of liquid Sr–Sb alloys as a function of composition at the temperatures indicated in the figure.

4. Discussion of the conductivities of the liquid systems

In figure 5 the conductivities of the liquid systems Mg–Bi, Mg–Sb, Sr–Bi and Sr–Sb are plotted. The data for Sr–Sb are adopted from the work by Verbrugge and Van Zytveld [16]. Qualitatively the behaviour of all the systems is very similar. There is a sharp and deep conductivity minimum at the composition with 40 at.% pnictide. This corresponds to compound formation according to the octet rule. For Sr–Sb this result is remarkable as the solid compound Sr_3Sb_2 does not persist up to the liquidus [8]. No indication is found for anion-cluster formation. If such clusters are formed one expects deviations from the simple octet rule. In this respect the alkaline-earth–pnictide alloys behave quite differently from the alloys of the alkali metals with the post-transition group IV and V elements mentioned in the introduction.

Overall, the conductivities decrease in the order Mg–Bi, Mg–Sb, Sr–Bi, Sr–Sb. In this comparison the peak values are not considered as they are not reliable (see [23] and remarks above). As the stoichiometries of all the systems are in accordance with the octet rule, it is interesting to consider the electronegativities. According to the Miedema scale [10], the electronegativity differences between the components are 0.70 for Mg–Bi, 0.95 for Mg–Sb,

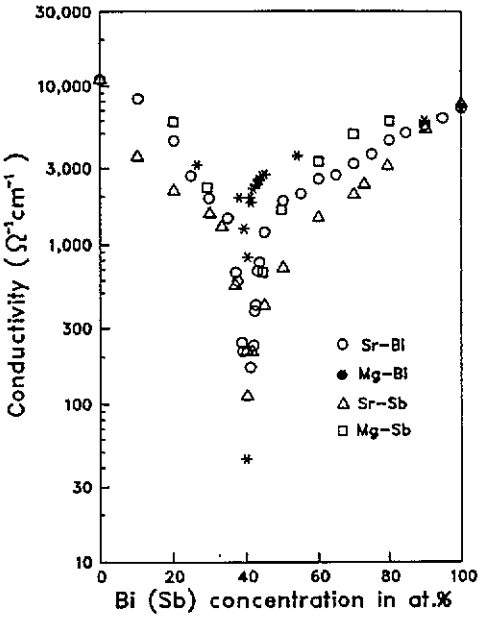

Figure 5. The conductivity σ of liquid Sr–Bi, Sr–Sb, Mg–Bi [1, 3] and Mg–Sb [16] alloys as a function of composition.

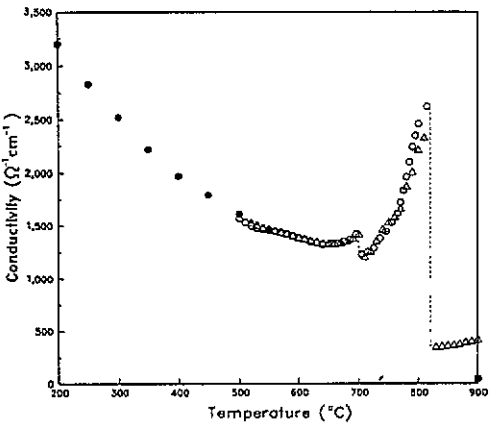

Figure 6. The conductivities σ of Mg_3Bi_2 as a function of temperature: ●, [11]; ■, [3]; ○, sample 1; △, sample 2.

1.75 for Sr–Bi and 2.00 for Sr–Sb, so there exists a monotonic relation between conductivity and electronegativity difference. This is in accordance with the rule of thumb stating that the density of states in the ionic (pseudo)gap becomes smaller as the electronegativity difference increases. Though the relation is monotonic, the actual values are out of proportion. From the electronegativities one expects the difference in conductivities between Mg–Bi and Sr–Bi to be much larger than that between Sr–Bi and Sr–Sb. A possible size effect works in the same direction [8]: as the electrons are predominantly in pnictide states, conduction occurs at least partially along pnictide–pnictide bonds. These paths become less effective when the transfer integrals between the pnictide valence orbitals are reduced. This happens when the ratio of the sizes of the alkaline-earth and pnictide atoms becomes too large.

5. Temperature dependence of the conductivity of Mg_3Bi_2

We now anticipate the results of the band-structure calculations presented in section 8. According to these calculations the Fermi level of the solid Mg_3Bi_2 is not in an energy gap and consequently Mg_3Bi_2 should be metallic. As far as the authors know this would be the first example of an alloy that is metallic in the solid state and semiconducting in the liquid state (indeed, a smaller increase of the resistivity on melting is found in several alloys, e.g. the Te–chalcogenide alloys, see [24]). An experimental verification is therefore highly desirable.

An extensive literature search revealed that metallic conductivity had been observed already by Grube *et al* in 1934 [11] and by Stepanow in 1912 [12]. Grube *et al* obtained resistivities in a wide composition range and in a temperature range from 50 up to 550 °C. We have checked the measurements of Grube *et al* and extended them through the melting

point up to 900 °C. As the conductivity for the liquid Mg_3Bi_2 alloys is very low, a four-probe method was appropriate. We used the same closed cell as for the liquid samples. This involves an experimental risk as good electrical contacts between electrodes and sample are not so easily established in the solid phase as they are in the liquid phase. We have therefore carefully checked the reproducibility, which prooved to be excellent. Mg_3Bi_2 experiences a phase transition from a low-temperature α phase to a high-temperature β phase (see below). Since we would also like to know the conducting behaviour during the phase transition from the α to the β phase, we controlled the temperature stability within ± 1 °C and set a step of 5 °C between the measuring points.

For a comparison with the data from the literature, the conductivities σ as a function of temperature for Mg_3Bi_2 alloys are plotted in figure 6. Our results are only slightly different from the older data determined by Grube *et al* [11] in the region of overlap. Moreover, two sets of our data from different samples between 500 °C and 750 °C are identical. However, a large discrepancy was found around the melting point, which may be due to the uncertainty in the composition. For the liquid Mg_3Bi_2 alloy, a value of the conductivity of about 413.8 Ω^{-1} cm^{-1} with positive temperature coefficient was found at 900 °C, which is much higher than the value determined by Enderby and Collings [3]. The inaccuracy of the conductivity may be caused by the same problem as met in the Sr–pnictide systems mentioned above. The results still indicate semiconducting behaviour. The maximum value of $d \ln \sigma / dT$, 3.87×10^{-3} K^{-1}, was obtained at 900 °C.

As plotted in figure 6, the electrical conductivity of the solid Mg_3Bi_2 alloy shows a continuous variation in behaviour as a function of the temperature, with the exception of a jump at 705 °C. Solid Mg_3Bi_2 alloy in the low-temperature range is more metallic. As the temperature increases up to 500 °C the conductivity σ goes down into the region of diffusive motion with a negative temperature coefficient. For 600 °C$< T <$ 650 °C, the conductivity σ tends to be constant. At 650 °C $d\sigma/dT$ becomes positive and remains so in the diffusive-motion region of the high-temperature solid phase. A jump in the conductivity occurs at approximately 705 °C, which is ascribed to the transition from the α phase to the β phase. The solid–liquid transition is quite distinct in the measurements and is observed at approximately 826 °C. These temperatures are in excellent agreement with phase-diagram data [17].

The conductivity of solid Mg_3Sb_2 was measured by Busch *et al* [22]. In contrast to Mg_3Bi_2 it exhibits a semiconducting behaviour. The differences between Mg_3Bi_2 and Mg_3Sb_2 will be discussed in section 8.

6. Comparison with amorphous films

It is interesting to compare our conductivity data with those obtained for amorphous films. Figure 7 shows the conductivities σ of amorphous Mg–Bi systems as a function of concentration. Data are taken from several publications [13–15]. Both the liquid and the amorphous materials show a very low and sharp minimum in the conductivity at the composition Mg_3Bi_2, typical for semiconducting behaviour. After annealing this minimum broadens considerably and the minimum conductivity increases up to nearly 1000 Ω^{-1} cm^{-1}, which is about two orders of magnitude larger than in the amorphous state. For comparison we have also included in figure 7 the results for the solid alloys [11], which are even more metallic. In the solid state only a small hump at 60 at.% Mg is left.

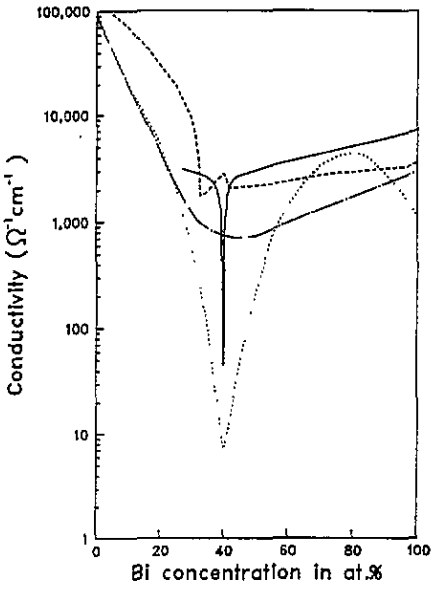

Figure 7. The conductivity σ of the Mg–Bi system:——, liquid alloys at 900 °C [1, 3]; - - - -, solid alloys at 250 °C [11]; ·····, amorphous films and — · —, annealed films [13].

7. Remarks on phase diagrams, crystal structures and technical aspects of the band-structure calculations

In strongly compound-forming liquid alloys a comparison with the solid state is often informative. This is particularly so when the composition of the liquid alloy is equal to that of a congruently melting phase. We have carried out band-structure calculations for Mg_3Bi_2 and Mg_3Sb_2 but before entering into a description of these calculations some remarks on the existing phases are appropriate.

Some confusion exists around the existence of compounds in the systems consisting of Mg and Sr on the one hand and Sb and Bi on the other hand. According to Massalski *et al* [17] in the two Mg-containing systems only the octet compounds Mg_3Bi_2 and Mg_3Sb_2 exist. Their structures have been determined by Zintl and Husemann [25]. In the case of the Sr-containing alloys discrepancies exist between the compositions of intermetallic compounds investigated crystallographically [26–30] and those mentioned in the phase diagram compilation by Massalski *et al* [17]. Unfortunately, no crystal structure determinations have been published for the Sr compounds most interesting for comparison with the liquid state, Sr_3Bi_2 and Sr_3Sb_2. Therefore we have carried out band-structure calculations for the two Mg alloys rather than for the Sr alloys. Eisenmann [31] has explained that the discrepancies and the lack of data may be caused by major problems of purity and definition of the solid compounds.

In both systems, Mg–Bi and Mg–Sb, the liquidus exhibits a narrow high cap around the composition with 60 at.% Mg. Phase transitions from a low-temperature α phase to a high-temperature β phase occur at 703 °C and 930 °C in the compounds Mg_3Bi_2 and Mg_3Sb_2, respectively. Unfortunately the crystal structure determinations pertain to the low-temperature α phase only. Investigation of the high-temperature phases might have given more insight into the properties of the liquid compounds.

The α phases, on which our band structure calculations are based, crystallize in the hexagonal La_2O_3-like structure [25, 32], space group $p\bar{3}m1$-D^3_{3d} (No 164 in the International Tables for X-ray Crystallography). The unit cell is shown in figure 8. It consists of one Mg atom at the 1a site (0,0,0), two equivalent Mg atoms at 2d sites $(\frac{1}{3}, \frac{2}{3}, Z_1)$ and $(\frac{2}{3}, \frac{1}{3}, \bar{Z}_1)$,

and two equivalent Bi (Sb) atoms at the 2d sites ($\frac{1}{3}$, $\frac{2}{3}$, Z_2) and ($\frac{2}{3}$, $\frac{1}{3}$, $\bar{Z}_2$). $Z_1 = 0.235$ and $Z_2 = 0.630$.

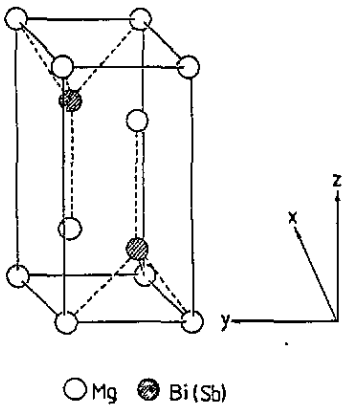

Figure 8. The crystal structure of α-Mg_3Bi_2 (or α-Mg_3Sb_2).

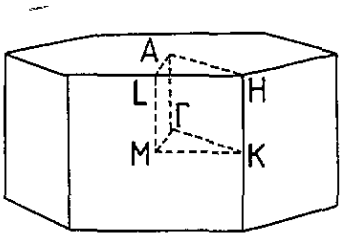

Figure 9. The first Brillouin zone of the hexagonal lattice showing the positions of high-symmetry points and lines.

The band-structure calculations of crystalline Mg_3Bi_2 and Mg_3Sb_2 were performed using the augmented spherical wave (ASW) method [33]. Scalar relativistic effects were included as described by Methfessel and Kuebler [34]. Spin–orbit interaction was included in the Hamiltonian for the Bi compound by adding the $L \cdot S$ operator. For the Mg atoms the 3s, 3d and 3p functions were used as the basis; for the Bi atoms the basis consisted of 6s, 6p and 6d functions and for the Sb atoms, 5s, 5p and 5d functions. Mg 4f, Bi 5f and Sb 4f functions were included in the internal summation of the three-centre contributions to the matrix elements. This can be regarded as treating f states as a perturbation.

The input parameters of the calculation are the atomic numbers, the crystal structure and the Wigner–Seitz radii, which are tabulated in table 1 for Mg_3Bi_2 and table 2 for Mg_3Sb_2.

Table 1. Input parameters of the band-structure calculations for Mg_3Bi_2. The Wigner–Seitz radii are in atomic units. Inserted empty spheres are indicated by ES.

		Atomic position			
Atom	Atomic number	x	y	z	WS radius
Mg(1)	12	0.000 00	0.000 00	0.000 00	3.697 777
Mg(2)	12	0.577 35	0.000 00	0.366 82	3.261 862
Mg(2)	12	0.288 68	0.500 00	1.221 20	3.261 862
Bi	83	0.577 35	0.000 00	1.017 90	3.261 862
Bi	83	0.288 68	0.500 00	0.570 10	3.261 862
ES	—	0.000 00	0.000 00	0.793 99	3.261 862
Lattice constants		$a = 4.666$ Å	$c = 7.401$ Å		$c/a = 1.586$

For the construction of a self-consistent potential, band-structure calculations have been performed at points on a regular mesh in an irreducible part of the Brillouin zone. The symmetry lines in the hexagonal Brillouin zone are shown in figure 9. We have used the symmetry notations of Miller and Love [35].

Table 2. Input parameters of the band-structure calculations for Mg_3Sb_2. The Wigner–Seitz radii are in atomic units. Inserted empty spheres are indicated by ES.

		Atomic position			
Atom	Atomic number	x	y	z	ws radius
Mg(1)	12	0.000 00	0.000 00	0.000 00	3.625 414
Mg(2)	12	0.577 35	0.000 00	0.371 54	3.198 029
Mg(2)	12	0.288 68	0.500 00	1.209 46	3.198 029
Sb	51	0.577 35	0.000 00	0.996 03	3.198 029
Sb	51	0.288 68	0.500 00	0.584 97	3.198 029
ES	—	0.000 00	0.000 00	0.790 50	3.198 029
Lattice constants		$a = 4.573$ Å	$c = 7.229$ Å		$c/a = 1.581$

8. Band structures of Mg_3Bi_2 and Mg_3Sb_2

Figure 10 shows the calculated band structure of Mg_3Sb_2 along the high-symmetry directions of the trigonal Brillouin zone. It is the band structure one expects for an octet compound. At low energies one finds bands of primarily Sb s character. Below the Fermi energy there is a complex of Sb p states with various degrees of admixture of metal state. Above the gap of about 0.12 eV, one finds a state of very delocalized character with metal s as largest contributor. The band gap is indirect with the top of the valence band at Γ and the bottom of the conduction band along the line M–L. The band structure of Mg_3Bi_2, as shown in figure 11, shows a different behaviour, especially around the Fermi energy. We find intersections of the bands with the Fermi level for most high-symmetry directions, i.e. it is a metal. The most noticeable differences as compared with Mg_3Sb_2 are around the Γ point and the Γ-A line. Since these are the regions in the Brillouin zone with the highest degeneracies it is plausible to assume that the differences between Mg_3Bi_2 and Mg_3Sb_2 are relativistic in origin (A lowering of the symmetry leads to orbital quenching and a consequent reduction of the importance of the spin–orbit interaction). In order to test this idea we show the band structure of Mg_3Bi_2 without the spin–orbit interaction in figure 12. The topologies of the valence and conduction bands agree much more closely now with those calculated for Mg_3Sb_2, but still one finds intersections of the top of the valence band around the Γ point with the Fermi energy as well as the bottom of the conduction band along the M-L line. Figure 13 shows the complete non-relativistic band structure of Mg_3Bi_2. The overlap of the valence and conduction bands has been slightly reduced as compared with the scalar-relativistic calculation in figure 12, but according to this calculation Mg_3Bi_2 should still be a semi-metal. Otherwise the band structure of Mg_3Bi_2 calculated without relativistic corrections (figure 13) bears a strong similarity to that of Mg_3Sb_2 (figure 10), which was calculated using mass-velocity and Darwin terms only. Note the strong upward shift of the lowest bands in this case since the mass-velocity and Darwin terms influence the Bi s states most strongly.

The differences between Mg_3Sb_2 and non-relativistic Mg_3Bi_2 are easily understood by the differences in electronegativity of the group-V elements involved. The same trend is for example found in the diminution of the band gaps in the series GaP, GaAs, GaSb. In conclusion, the differences between metallic Mg_3Bi_2 and semiconducting Mg_3Sb_2 originate from both the relativistic effects and the difference in electronegativity between Bi and Sb. To a certain extent this trend is the opposite of that found in CsAu, which is semiconducting due to relativistic effects [36].

We now address the question of the origin of the differences between liquid and solid Mg_3Bi_2. Since we have no calculation for the liquid available we can only speculate. A

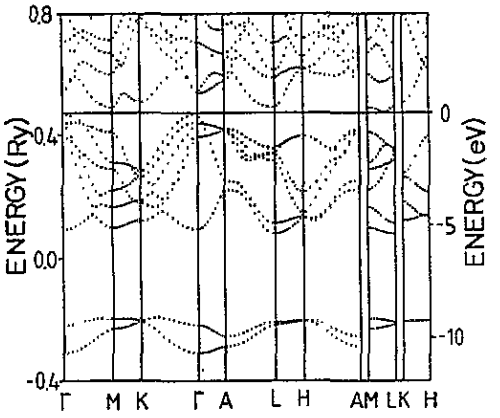

Figure 10. The band structure of Mg_3Sb_2. The full line at 0 eV corresponds to the Fermi energy.

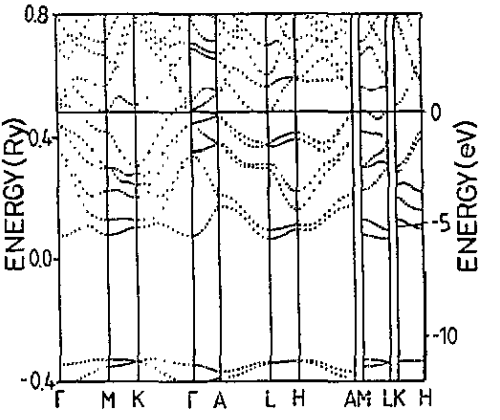

Figure 11. The band structure of Mg_3Bi_2.

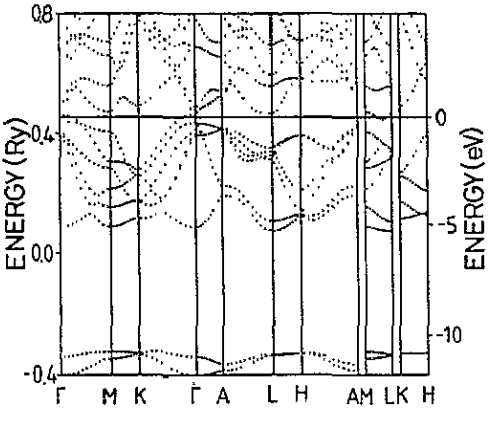

Figure 12. The scalar-relativistic band structure of Mg_3Bi_2.

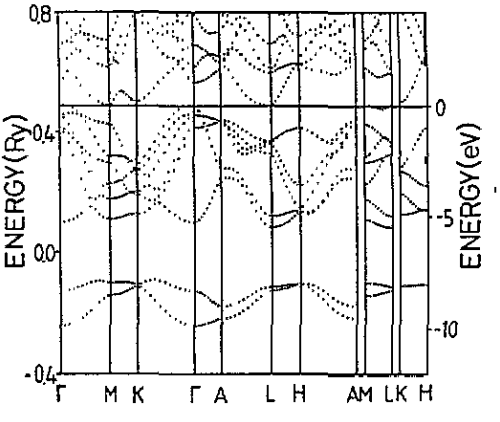

Figure 13. The non-relativistic band structure of Mg_3Bi_2.

first consideration would be the lowering of the symmetry of the system upon melting. This lowering of the symmetry will split degenerate eigenstates and hence reduce the effect of the spin–orbit interaction. Since Mg_3Bi_2 calculated without spin–orbit interaction (figure 12) is at least a semi-metal it is clear that this effect alone cannot be responsible for the differences between liquid and solid. Another possibility is the following. The coordination of the atoms in the solid is unusual, with a seven fold coordination of the metal. It is quite imaginable that a more regular coordination will increase the gap to positive values, but it is impossible to combine a regular coordination in a compound with stoichiometric composition 3:2 with the constraints imposed by lattice periodicity. Since liquids (and amorphous films) do not suffer from this constraint, they may adopt a more regular coordination and thus obtain semiconducting properties. Against this explanation is the occurrence of the high-temperature crystalline phase of Mg_3Bi_2, which shows properties of a semiconductor as well. Since nothing is known about the crystal structure, the amount of disorder etc of this phase, we do not want to derive any conclusions from it, however.

9. Final Remarks

The alloys of Mg and Sr, on the one hand, and Sb and Bi, on the other hand, form a homogeneous group of systems. In the liquid state their resistivities exhibit a quite similar behaviour. The simple octet compound is strongly dominant in all liquid systems. The differences in electrical conduction of the liquid systems can be understood in terms of electronegativity and size effects. Solid Mg_3Bi_2 is a metal. The difference from solid Mg_3Sb_2, which is a semiconductor, can be understood from relativistic effects and electronegativities. The metal–non-metal transition at the melting point of Mg_3Bi_2 is remarkable as it is the solid phase that exhibits metallic conduction. Suggestions have been put forward to explain this phenomenon but they are all somewhat speculative.

Acknowledgments

The authors gratefully acknowledge the technical assistance of F van der Horst, J F M Wieland, H Bron and R Kinderman during the measurements. They also thank D M Verbrugge and J B van Zytveld for their permission to quote from their results prior to publication.

This work forms part of the research programme of the Stichting voor Fundamenteel Onderzoek der Materie (Foundation for Fundamental Research on Matter, FOM) and was made possible by financial support from the Nederlandse Organisatie voor Wetenschappelijk Onderzoek (Netherlands Organisation for Scientific Research, NWO).

References

[1] Ilschner B R and Wagner C 1958 *Acta Metall.* **6** 712
[2] Glazov V M and Situlina O V 1969 *Akad Nauk. SSSR Chem.* **167** 587
[3] Enderby J E and Collings E W 1970 *J. Non-Cryst. Solids* **4** 161
[4] Egan J J 1959 *Acta Metall.* 7 560
[5] Darken L S 1967 *Trans. Metall. Soc. AIME* **239** 80
[6] Weber M, Steeb S and Lamparter P 1979 *Z. Naturf.* a **34** 1398
[7] Boos A and Steeb S 1977 *Phys. Lett.* **63A** 333
[8] van der Lugt W and Geertsma W 1987 *Can. J. Phys.* **65** 326
[9] van der Lugt W 1991 *Phys. Scr.* T **39** 372
[10] Miedema A R, Boom R and de Boer F R 1975 *J. Less-Common Met.* **41** 283
[11] Grube G, Mohr L and Bornhak R 1934 *Z. Elektrochem.* **40** 143
[12] Stepanow N J 1912 *Z. Anorg. (Allg.) Chem.* **78** 1
[13] Ferrier R P and Herrell D J 1969 *Phil. Mag.* **19** 853
[14] Ferrier R P and Herrell D J 1970 *J. Non-Cryst. Solids* **4** 338
[15] Sik M J and Ferrier R P 1974 *Phil. Mag.* **29** 877
[16] Verbrugge D M and van Zytveld J B 1993 *J. Non-Cryst. Solids* **156/158** 736
[17] Massalski T B, Murray J L, Bennett L H, Baker H and Kaprzak L 1986 *Binary Alloy Phase Diagrams* (Metal Park, OH; American Society for Metals)
[18] van Zytveld J B, Enderby J E and Collings E W 1972 *J. Phys. F: Met. Phys.* 2 73
[19] Xu R, Kinderman R and van der Lugt W 1991 *J. Phys.: Condens. Matter* 3 127
[20] Meijer J A, Vinke G J B and van der Lugt W 1986 *J. Phys. F: Met. Phys.* **16** 845
[21] Xu R, de Jonge T and van der Lugt W 1992 *Phys. Rev.* B **45** 12 788
[22] Busch G, Hulliger F and Winkler U 1954 *Helv. Phys. Acta* **27** 249
[23] Enderby J E 1974 *Amorphous and Liquid Semiconductors* ed J Tauc (New York: Plenum) p 409
[24] Enderby J E and Barnes A C 1990 *Rep. Prog. Phys.* **53** 85
[25] Zintl E and Husemann E 1933 *Z. Phys. Chem.* **20** 272
[26] Eisenmann B and Deller K 1975 *Z. Naturf.* b **30** 66

[27] Martinez-Ripoll M, Haase A and Brauer G 1973 *Acta Crystallogr.* B **29** 1715
[28] Martinez-Ripoll M and Brauer G 1973 *Acta Crystallogr.* B **29** 2717
[29] Deller K and Eisenmann B 1976 Z. *Naturf.* b **31** 1146
[30] Eisenmann B 1979 Z. *Naturf.* b **34** 1162
[31] Eisenmann B 1992 private communication
[32] Gottfried C and Schossberger F 1933–1935 *Structure Report* **3** 48
[33] Williams A R, Kuebler J and Gelatt G D Jr 1979 *Phys. Rev.* B **19** 6094
[34] Methfessel M and Kuebler J 1982 *J. Phys. F: Met. Phys.* **12** 141
[35] Miller S C and Love W F 1967 *Tables of Irreducible Representations of Space Groups and Co-representations of Magnetic Space Groups* (Boulder, CO: Pruett) p 131
[36] Christensen N E and Kollar J 1983 *Solid State Commun.* **46** 727